Mechanics and Energetics of Electromembranes

Hadrien Bense,[1,2] Benoit Roman,[1,2] Jacco Snoeijer,[3] and Bruno Andreotti[4]

Abstract

The recent discovery of electroactive polymers has shown great promises in the field of soft robotics and was logically followed by experimental, numerical, and theoretical developments. Most of these studies were concerned with systems entirely covered by electrodes. However, there is a growing interest for partially active polymers, in which the electrode covers only one part of the membrane. Indeed, such actuation can trigger buckling instabilities and so represents a route toward the control of three-dimensional shapes. Here, we study theoretically the behavior of such partially active electroactive polymer. We address two problems: (1) the electrostatic elastica including geometric nonlinearities and partially electroactive strip using a variational approach. We propose a new interpretation of the equations of deformation, by drawing analogies with biological growth, in which the effect of the electric voltage is seen as a change in the reference stress-free state. (2) We explain the nature of the distribution of electrostatic forces on this simple system, which is not trivial. In particular, we find that edge effects are playing a major role in this problem.

Keywords: electromembrane, buckling, electroactive polymers

Introduction

SOFT ROBOTICS IS A NEW rapidly developing scientific field. It aims at designing compliant robots able to move in topographically complex environments or able to manipulate fragile objects.[1–3] Potential applications range from artificial heart[4] to bioinspired locomotion[5,6] or haptic interfaces for virtual reality where the user feels a feedback force from the interface that he manipulates.[7]

Electroactive polymers (EAPs) offer a promising candidate for building such soft robots. Their large reversible deformations (tens of percent strains) under an applied electric field triggered a huge interest in academic laboratories over the world.[8] Several types of electroresponsive polymers have been described in the literature, such as anionic, ferroelectrics, liquid-crystalline, and electrorheological.[9–11] In this article, we are specifically interested in EAPs, which are the most simple and inexpensive in terms of manufacturing.[12] In their simplest form, EAPs are indeed composed of a thin membrane of elastomer covered by two conductive compliant layers. When an electric field is applied, the electrodes of this soft capacitor are attracted to each other, resulting into in-plane isotropic strain. A wide range of applications of EAPs have been proposed, they include: robots actuation,[13–16] rotational motors,[17] flapping wings,[18,19] valves,[20,21] actuators for biological cells,[22] Braille displays,[7,23,24] tunable lenses,[25,26] artificial chromatophores,[27,28] tunable diffracting surfaces,[29] or phase shifters for microwave communications.[30] As in the case of piezo-electric ceramics, this electromechanical coupling can potentially be reversed in EAPs: an electric power may be harvested from mechanical strain,[31–34] or conversely, the device may work as a mechanical sensor.[35,36]

In this article, we investigate theoretically the behavior of an EAP in the case where its surfaces are not entirely covered by conductive electrodes. This situation is interesting as it leads to buckling instabilities and is a way to obtain out-of-plane shapes[37–39] through the nonlinear response of the structure. The aim of this article was to clarify three questions that arise in this problem. Namely, the literature usually considers membranes completely covered by conductive electrode, and one usually models electrostatic effects by an electrostatic pressure, which is twice the actual value of the pressure,[8] in the case of

[1]Physique et Mécanique des Milieux Hétérogènes (PMMH), CNRS, ESPCI Paris, PSL Research University, Paris, France.
[2]Sorbonne Universite, Universite Paris Diderot, Paris, France.
[3]Physics of Fluids Group, Faculty of Science and Technology, Mesa+ Institute, University of Twente, Enschede, The Netherlands.
[4]Laboratoire de Physique de l'Ecole Normale Supérieure, ENS, Université PSL, CNRS, Sorbonne Université, Université de Paris, Paris, France.

incompressible elastomers ($\nu = 1/2$). In this article, we will refer to this description as "Pelrine's approach." The argument is based on the superposition of an isotropic stress (which has no effect on an incompressible material) to the actual electrostatic pressure on the faces.[40] The questions we would like to address are: (1) Does this argument apply to cases where electrostatics is only active on a portion of the plate? (2) Does the argument remain valid for nonplanar buckled states? (3) Can we determine the real distribution of electrostatic forces and relate it to the electromechanical equilibrium of a strip? Indeed, standard approaches[40,41] provide a calculation of the mechanical stresses in the material resulting from the electrostatic loading, and even to adequately predict the onset of wrinkling and its possible evolution in pull-in instability[42] but do not provide the real distribution of electrostatic forces from which they originate.

In this article, we use a variational approach to clarify the nature of electrostatic forces acting on an electroactive membrane. Our aim is to make an explicit link between variational and stress-based approaches of the problem (i.e., a direct description of electrostatic forces on the elastic system), in a detailed way. Particular attention is paid to the edge of the electrode, from the mechanical and the electrostatic point of view. We show that the usually used Pelrine's approach of electromechanical coupling extends to these nonuniform activations in the planar case, but that it misses a modification of the bending stiffness due to electrostatic loading. We propose here an alternative analogy, where the EAP is seen as undergoing a change in its reference stress-free state when submitted to electric voltage. Plasticity, biological growth, or chemical swelling are other cases where the reference state of the material evolves, and we suggest that electroactive materials may be seen as analogous to these situations.

The article is organized as follows: In the Variational Approach section, the nonlinear out-of-plane equilibrium equations for a partially electroactive plate are derived from a variational approach, in the asymptotic limit of thin membranes. These equations involve strain discontinuities at the boundary of the electrodes, and we show how they lead to electrostatically induced buckling. We discuss an analogous description in terms of a modification of the rest state. In the Stress-Based Approach section, we turn to stress-based approaches to analyze the previous results in term of force distribution. We discuss the "double electrostatic pressure" description used in a large body of literature on electroactive materials and comment on the Maxwell stresses and their interpretation. We finally derive the distribution of electrostatic forces directly applied by charges on the elastic plate and show the importance of electrostatic edge effects and finally conclude in the Concluding Remarks section.

Variational Approach

We start by defining the model situation that we will use throughout the article to discuss electroactive coupling. Although we consider here the specific plane strain geometry of a strip, and later use specific boundary conditions for the sake of simplicity, the discussion presented is more general.

Parametrization

We consider the problem of a thin strip of a dielectric elastic material whose thickness in the reference state is noted H and whose width is W. A portion of the strip has conductive
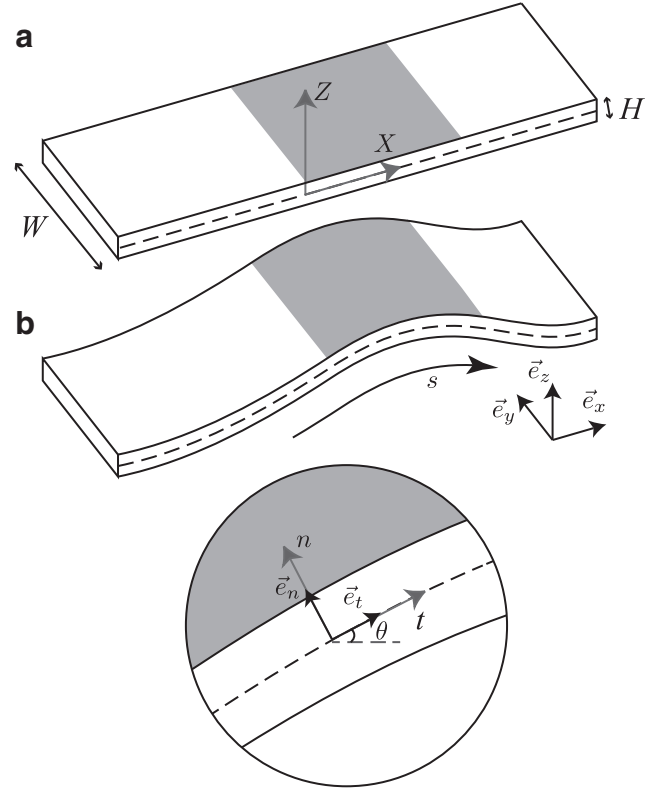

FIG. 1. Schematics of the elastic strip partially covered with compliant electrodes. **(a)** Coordinates of the reference state. **(b)** Coordinates in the current state.

faces (represented in gray in Fig. 1), which will be submitted to a difference in electric potential U (Fig. 1). We neglect any stiffening due to the presence of the conductive material. We start by a general derivation of the equations and illustrate later (in the Variations section) the buckling for a case with specific boundary conditions (the clamped–clamped case, chosen for simplicity). We restrict ourselves to the situation where the strip is not strained along the transverse Y direction (plane strain configuration). In the reference state, the coordinates X and Z, respectively, run along and across the membrane (Fig. 1a). We will assume small strain but follow a geometrically fully nonlinear approach, equivalent to Euler's elastica theory.[43] This beam geometry, although idealized in comparison with real situations, illustrates the main points of the problem and reveals a nontrivial force distribution.

For the deformed configuration, we adopt a curvilinear description for the centerline position $\mathbf{r}_0(s)$, where s is the curvilinear coordinate running along the centerline (Fig. 1b). The local orientation is defined by the tangential and normal unit vectors

$$\mathbf{t} = \frac{d\mathbf{r}_0}{ds} = (\cos\theta, \sin\theta), \quad \mathbf{n} = \frac{d\mathbf{t}}{d\theta} = (-\sin\theta, \cos\theta). \quad (1)$$

The position in the transverse direction is denoted by the coordinate n, so that any point inside the membrane is described by

$$\mathbf{r} = \mathbf{r}_0(s) + n\mathbf{n}(s) \quad \Rightarrow \quad \frac{d\mathbf{r}}{ds} = (1 - n\kappa)\mathbf{t}, \quad \frac{d\mathbf{r}}{dn} = \mathbf{n}, \quad (2)$$

where we introduce the curvature $\kappa = d\theta/ds$. From these transformations, one derives the size of an area element as

$$d^2\mathbf{r} = dsdn(1 - n\kappa). \tag{3}$$

In the reference state, the curvilinear coordinate is noted S; it is assumed flat. In the slender limit, it is useful to introduce the tangential strain averaged over the cross section of the membrane e_t, which determines the stretching

$$ds = (1 + e_t)dS, \tag{4}$$

where $dS = dX$ is the curvilinear coordinate in the reference state. Similarly, we define the averaged normal strain $e_n(S)$, defined by

$$h = (1 + e_n)H, \tag{5}$$

where h is the thickness of the strip in the deformed configuration.

It will turn out convenient to treat the local angle also as a function of the reference coordinate, $\theta(S)$, so that the curvature becomes

$$\kappa \equiv \frac{d\theta}{ds} = \frac{1}{1 + e_t}\frac{d\theta}{dS} \simeq \frac{d\theta}{dS}. \tag{6}$$

The approximation in the final step is due to the slender body assumption, that is, on the small curvature, $(H\kappa)^2 \ll 1$, so that we can neglect terms involving products of both κ and e_t or e_n.[43]

Elasticity

In linear elasticity, the total elastic energy is obtained by integrating over the reference volume as

$$F_e = \frac{E}{(1 + \nu)}\int d^3\mathbf{X}\left(\frac{1}{2}\varepsilon_{ij}\varepsilon_{ij} + \frac{\nu}{2(1 - 2\nu)}(\varepsilon_{kk})^2\right), \tag{7}$$

where ε_{ij} is the linear strain tensor, defined by:

$$\varepsilon_{ij} = \frac{1}{2}\left(\frac{\partial u_i}{\partial X_j} + \frac{\partial u_j}{\partial X_i}\right), \tag{8}$$

and E the Young modulus of the polymer and ν the Poisson's ratio.

Minimization of these equations with respect to the displacement field gives the equations of linear elasticity.

We now follow the standard slender-body reduction of these equations (Euler–Bernoulli assumption), as described, for example, in Audoly and Pomeau,[43] which gives:

$$\varepsilon_{XX} = e_t - \kappa Z, \quad \varepsilon_{ZZ} = e_n + \frac{\nu}{1 - \nu}\kappa Z, \quad \varepsilon_{XZ} = 0, \tag{9}$$

where e_t, e_n and κ as defined above. We recall that we have assumed a plane strain configuration, so that $\varepsilon_{YY} = \varepsilon_{YZ} = \varepsilon_{XY} = 0$. In the usual development of the membrane equations, one makes use of the fact that the normal stress $\tau_{ZZ} = 0$, which is used, for example, to eliminate the normal strain e_n. In the present context, however, this is not allowed since the

charged conductors will exert a normal force on the membrane. Hence, we need to retain e_n as a variable. Now, we integrate the elastic energy over the thickness of the layer, inserting Equation (9) in Equation (7), which yields the elastic energy per unit membrane area,

$$\frac{E}{(1 + \nu)}\int_{-H/2}^{H/2}dZ\left(\frac{1}{2}\left(\varepsilon_{XX}^2 + \varepsilon_{ZZ}^2\right) + \frac{\nu}{2(1 - 2\nu)}\left(\varepsilon_{XX} + \varepsilon_{ZZ}\right)^2\right)$$

$$= \frac{1}{2}Y\left(e_t^2 + \frac{2\nu}{1 - \nu}e_ne_t + e_n^2\right) + \frac{1}{2}B\theta'^2,$$

where the prime is used for the derivative with respect to S. We have introduced the effective stretching modulus Y and the bending modulus B, defined as:

$$Y = \frac{(1 - \nu)EH}{(1 - 2\nu)(1 + \nu)} \quad \text{and} \quad B = \frac{EH^3}{12(1 - \nu^2)}. \tag{10}$$

Finally, the elastic energy per unit width, which is a functional of the fields $e_t(S)$, $e_n(S)$ and $\theta(S)$, reads:

$$F_e = \int dS\left[\frac{1}{2}Y\left(e_t^2 + \frac{2\nu}{1 - \nu}e_ne_t + e_n^2\right) + \frac{1}{2}B\theta'^2\right]. \tag{11}$$

The first term represents the in-plane energy due to tangential and normal strain, whereas the second term represents the plate bending energy.

Electrostatics

The two conductive electrodes form a capacitor maintained at constant potential difference U. Denoting by C the capacitance, the electrostatic energy reads $\frac{1}{2}CU^2$. Elastic deformations of the membrane lead to a change in the capacitance by δC. The source that maintains the electrical potential difference U constant brings a charge $U\delta C$ to the capacitor, and as such, the capacitor receives a work $U^2\delta C$ performed by the source. By consequence, at constant potential, the total electrostatic free energy to be minimized[44] is $F_U = -\frac{1}{2}CU^2$. To explicitly perform the minimization with respect to the elastic degrees of freedom, it is convenient to express the energy in terms of the electrostatic potential ϕ. Namely, we can then write as a volume integral over the current state

$$F_U = -\frac{1}{2}\int d^3\mathbf{x}\varepsilon|\nabla\phi|^2, \tag{12}$$

where ε is the permittivity of the membrane. We anticipate that $\nabla\phi = 0$ everywhere outside the membrane, which implies that we neglect the energetic contribution due to fringe effects near the edge of the plate. Hence, the integral in Equation (12) runs over the volume of the membrane, in the current state. Minimization of the electrostatic energy with respect to the potential ϕ yields the expected field equation $\nabla^2\phi = 0$, to be solved inside the deformed membrane.

Within the same slender body asymptotics $[(h\kappa)^2 \ll 1]$ as used for the strain field, the gradient of the potential is

approximately constant inside the thin gap and points normal to the surface. We therefore seek a solution of the form

$$\phi = \frac{U}{h}\left(n + \frac{h}{2}\right) + (h\kappa)\phi_1(n, s), \tag{13}$$

where n is the local coordinate normal to the surface and we recall that $h = (1 + e_n)H$, and $\phi_1(n, s)$ a function that remains to be determined. Note the similarity with the expansion (9) for the strain field, which also consists of a solution corresponding to a flat membrane complemented with a curvature correction.

To obtain explicit expressions, we now need to express the gradient $\nabla\phi$ and the Laplacian $\nabla^2\phi$ in terms of the curvilinear coordinates s and n. This can be achieved formally through the transformation defined by Equation (2), which gives

$$\nabla\phi = \frac{\partial\phi}{\partial n}\mathbf{n} + \frac{1}{1 - n\kappa}\frac{\partial\phi}{\partial s}\mathbf{t}, \tag{14}$$

$$\nabla^2\phi \simeq \frac{\partial^2\phi}{\partial n^2} - \kappa\frac{\partial\phi}{\partial n}, \tag{15}$$

where for the Laplacian we retained only the leading order term in κ; this term originates from $\mathbf{t} \cdot \partial\mathbf{n}/\partial s = -\kappa$. We now insert the expansion (13) in $\nabla^2\phi = 0$, which gives to leading order:

$$\nabla^2\phi \simeq -\kappa\frac{U}{h} + (h\kappa)\frac{\partial^2\phi_1}{\partial n^2} = 0. \tag{16}$$

This equation governing the curvature correction ϕ_1 can be integrated twice to yield

$$\phi = U\left[\frac{n + \frac{h}{2}}{h} + \frac{1}{2}\frac{(n + \frac{h}{2})(n - \frac{h}{2})}{h^2}(h\kappa)\right], \tag{17}$$

where we imposed boundary conditions $\phi = U$ and 0 at $n = h/2$ and $n = -h/2$, respectively. Now that we have solved for the field inside the membrane, including the correction due to curvature, we can evaluate the volumetric energy density

$$-\frac{\varepsilon}{2}|\nabla\phi|^2 = -\frac{\varepsilon}{2}\frac{U^2}{h^2}[1 + n\kappa]^2. \tag{18}$$

Once again, we integrate this across the membrane, but we need to bear in mind that the area element also contains a curvature correction, $d^2\mathbf{r} = dsdn(1 - n\kappa)$, as derived in Equation (3). With this, we derive the electrostatic energy density per unit surface of the membrane:

$$-\int_{-h/2}^{h/2} dn(1 - n\kappa)\frac{\varepsilon}{2}|\nabla\phi|^2 = -\frac{\varepsilon}{2}\frac{U^2}{h}\left[1 - \frac{1}{12}(h\kappa)^2\right]. \tag{19}$$

It is worth noting that the same expression can be recovered from the capacity of the capacitor formed by two coaxial cylinders, which reads:

$$C = \frac{2\pi\varepsilon w}{\ln\left(\frac{1 + \kappa h/2}{1 - \kappa h/2}\right)}. \tag{20}$$

Indeed, the electrostatic energy per unit perimeter $-\frac{1}{2}CU^2/(2\pi/\kappa)$ when expanded for small curvature $\kappa h \ll 1$ leads to Equation (19).

We thus find the "slender" expression for the electrostatic energy (per unit width of the plate):

$$F_U = -\int ds\,\frac{\varepsilon}{2}\frac{U^2}{h}\left[1 - \frac{1}{12}(h\kappa)^2\right]. \tag{21}$$

The first term represents the energy stored in a plane capacitor with conductors separated by a distance h. It is proportional to the surface—we recall that F_U is written per unit membrane width—and is therefore analogous to a surface tension[45] but with a negative sign, similar to what is observed in electrowetting.[46]

Moreover, in analogy to the elastic energy [Eq. (11)], the electrostatic energy represents a bending rigidity as can be seen from the term~κ^2. The associated electrostatic bending modulus is

$$B_U = \frac{\varepsilon U^2 h}{12} \simeq \frac{\varepsilon U^2 H}{12}, \tag{22}$$

where in the remainder we will keep the leading order in strain ($h \simeq H$). This electrostatic stiffening may also be computed using the Maxwell stress tensor (Appendix A1).

Electrostatics is naturally expressed in Eulerian coordinates. When combined with the elastic formulation, however, it is important to bring this to Lagrangian coordinates. Using the transformations discussed above, this gives

$$F_U = -\frac{\varepsilon}{2}\frac{U^2}{H}\int dS\,\frac{1 + e_t}{1 + e_n} + \int dS\,\frac{1}{2}B_U\theta'^2. \tag{23}$$

Like the elastic energy [Eq. (11)], F_U is now a functional of $e_t(S)$, $e_n(S)$, and $\theta'(S)$. Note that for the bending term we neglect higher order corrections in e_t, e_n, and κH.

Variations

For the sake of simplicity, we choose here specific boundary conditions. We assume that the position of both ends of the strip is fixed. In particular, the end point position, measured from the origin reads:

$$\mathbf{r}_{\text{end}} = \int dS(1 + e_t)\mathbf{t}. \tag{24}$$

This constraint will be imposed with a Lagrange multiplier, $\mathbf{f}$, which in fact represents the load applied at the end of the plate. The total energy to be minimized then reads

$$F = F_e + F_U = \int dS\,\mathcal{F}(e_t, e_n, \theta), \tag{25}$$

with the surface density of energy given by

$$\mathcal{F}(e_t, e_n, \theta) = \frac{1}{2} Y \left(e_t^2 + \frac{2\nu}{1-\nu} e_n e_t + e_n^2 \right) + \frac{1}{2}(B + B_U)\theta'^2$$

$$- \frac{\varepsilon}{2} \frac{U^2}{H} \frac{1+e_t}{1+e_n} - (1+e_t)\mathbf{f} \cdot \mathbf{t}, \qquad (26)$$

where this expression must be used with $B_U = 0$ and $U = 0$ in the portion of the strip that is not covered by the electrode.

The equilibrium equations are obtained by variation of θ, e_t, and e_n. This gives the set of equations

$$\frac{\delta F}{\delta \theta(S)} = -(B + B_U)\theta'' - (1+e_t)\mathbf{f} \cdot \mathbf{n} = 0, \qquad (27)$$

$$\frac{\delta F}{\delta e_n(S)} = Y \left(e_n + \frac{\nu}{1-\nu} e_t \right) + \frac{\varepsilon}{2} \frac{U^2}{H} \frac{1+e_t}{(1+e_n)^2} = 0, \qquad (28)$$

$$\frac{\delta F}{\delta e_t(S)} = Y \left(e_t + \frac{\nu}{1-\nu} e_n \right) - \frac{\varepsilon}{2} \frac{U^2}{H} - \mathbf{f} \cdot \mathbf{t} = 0. \qquad (29)$$

The terms involving B_U and U are only present in the area covered by electrodes. These equations are valid for large displacement as they include the complete geometric nonlinearities and can therefore be applied to realistic EAPs. In the following, we will for simplicity consider the small strain limit and replace $1 + e_n \simeq 1$ and $1 + e_t \simeq 1$.

Equations (29) and (28) are in fact a force balance projected along the normal and tangential direction and provide the equations governing the normal and tangential strain,

$$\mathcal{Y} \left(e_n + \frac{\nu}{1-\nu} e_t \right) = -H\mathcal{P}, \qquad (30)$$

$$T \equiv \mathbf{f} \cdot \mathbf{t} = \mathcal{Y} \left(e_t + \frac{\nu}{1-\nu} e_n \right) - H\mathcal{P}. \qquad (31)$$

Here, we defined $T \equiv \mathbf{f} \cdot \mathbf{t}$ as the membrane tension (induced by the imposed force at the edge), and $\mathcal{P}$ as the electrostatic pressure, defined as the usual attractive pressure between two parallel conducting plates

$$\mathcal{P} = \frac{\varepsilon}{2} \frac{U^2}{H^2}. \qquad (32)$$

Usually, in plate or beam mechanics, one is not interested in the normal strain. We therefore eliminate e_n and obtain the equation governing the strain e_t:

$$T = \frac{EH}{1-\nu^2} e_t - \frac{1}{1-\nu} H\mathcal{P}. \qquad (33)$$

The total tension consists of the elastic tension of the membrane (first term), and a compressive (negative) tension induced by electrostatics (second term). While this equation for e_t is the most important for the beam, we will for later reference also compute the normal strain e_n, which reads

$$\frac{EH}{1-\nu^2} e_n + \frac{1}{1-\nu} H\mathcal{P} = -\frac{\nu}{1-\nu} T. \qquad (34)$$

Again, Equations (33) and (34) are also valid in the regions that are free of electrode, by using $\mathcal{P} = 0$.

Interestingly, at the transition between the conductive zone and the noncovered membrane, $\mathcal{P}$ exhibits a discontinuity since the electrostatic pressure $\mathcal{P}$ drops to zero outside the electrodes. But since $T = \mathbf{f} \cdot \mathbf{t}$ is continuous, this implies that there must be a discontinuity of the strain e_t and e_n at the boundary of the electrode. Following Hooke's law, this also implies a discontinuity of the elastic stress, whose physical origin will be discussed in the Force Transmitted by Surface Charges section and in the Edge Effects section.

We now turn our attention to the bending equation (27). In the small strain approximation, it then reduces to the standard elastica equation,[47]

$$(B + B_U)\theta'' + \mathbf{f} \cdot \mathbf{n} = 0, \qquad (35)$$

where the only modification due to electrostatics is the additional bending rigidity B_U, present in the part covered by electrodes. We also find that the torque $(B + B_U)\theta'$ is continuous across the edges of the electrode and therefore that the curvature θ' is either null or discontinuous at this boundary. It is instructive to estimate here the relative magnitude of the electrostatic added stiffness B_U by noting that $B_U/B = 2\mathcal{P}/E(1-\nu^2)$ is on the order of the strains (e_n, e_t) in the material, assumed to be small in the previous derivation. However, for practical cases where the stretching might be significant, the electrostatic bending rigidity needs to be taken into account.

As a summary, the equilibrium equations for this electrostatically activated beam are

$$(B + B_U)\theta'' + \mathbf{f} \cdot \mathbf{n} = 0$$

$$T \equiv \mathbf{f} \cdot \mathbf{t} = \frac{EH}{1-\nu^2} e_t - \frac{1}{1-\nu} H\mathcal{P},$$

where we emphasize that these equations are valid everywhere on the strip, taking $(B_U = 0, \mathcal{P} = 0)$ on parts that are not covered by electrodes. However, we remind the reader that the discontinuities in $\mathcal{P}$ and B_U at the boundaries of the electrode lead to discontinuities of strains e_t, e_n, and curvature θ'.

Equivalent growth model

An alternative way to write the equilibrium for the strain [Eqs. (33) and (34)] is the form

$$\frac{EH}{1-\nu^2}(e_t - e_t^0) = T. \qquad (36)$$

$$\frac{EH}{1-\nu^2}(e_n - e_n^0) = -\frac{\nu}{1-\nu} T, \qquad (37)$$

with

$$e_t^0 = (1+\nu)\frac{\mathcal{P}}{E}; \quad e_n^0 = -(1+\nu)\frac{\mathcal{P}}{E}. \qquad (38)$$

Written in this way, these equations allow another interpretation of the electrostatic loading: applying a voltage is equivalent to defining a new reference state (e_t^0, e_n^0), where by reference state we mean the state attained when there is no external mechanical loading T. This situation is similar to cases of inelastic strain, such as those produced by growth or plastic deformation, which effectively redefines the reference state. Hence, the electrostatic loading can be seen as a modification of the rest length of the strip and providing a new bending rigidity $B + B_U$.

Geometrically nonlinear equations and buckling instability

To illustrate how the electrostatic loading enters the equations, let us for example study a simple but geometrically nonlinear problem, namely the electrostatically induced buckling instability where the membrane has its two ends clamped. Under an imposed potential U on the electrode, the straight solution $\theta(S) = 0$ remains a solution. For this initially flat state $\mathbf{t} = (1, 0)$ and Equation (33) implies that e_t is piecewise constant. Imposing the constraint of no edge displacement, then implies $\int e_t dS = e_{t,U} L_U + e_{t,0}(L - L_U) = 0$, where L_U is the portion of the membrane that is covered by the electrode and L is the total length. Then, Equation (33) implies that the flat state comes with a compressive tension

$$T = -\frac{1}{1-\nu} H\mathcal{P} \frac{L_U}{L}. \tag{39}$$

We see that the magnitude of this compressive force increases with the potential U and depends on the fraction L_U/L that is covered by the electrode. Within the viewpoint presented in the Equivalent Growth Model section, this compression has a very simple interpretation, as the strip can be seen as taking a new rest state, which becomes longer (and stiffer) in the electrode area; for fixed edges, this implies a global compression. The linear stability analysis of Equations (33) and (35) around this solution shows that this system is unstable under classical buckling (see Bense et al.[37] for a study of an axisymmetric case for this buckling problem). For the simplifying case where the entire membrane with length L is covered with the electrodes, the electrostatic pressure, and thus e_t and B_U, are uniform along the membrane. The buckling threshold can be identified for small perturbations of the elastica equation, which becomes

$$\theta'' + \frac{H\mathcal{P}}{(1-\nu)(B+B_U)}\theta = 0. \quad \theta(0) = \theta(L) = 0 \tag{40}$$

Defining Euler's critical load $T_c = 4\pi^2(B+B_U)/L^2$ for clamped–clamped boundary conditions, we thus find

$$\frac{H\mathcal{P}}{(1-\nu)(B+B_U)} = 4\pi^2/L^2. \tag{41}$$

This determines the critical electrostatic pressure $\mathcal{P}$, and thus the critical potential U, for buckling.

Stress-Based Approach

We have established above the conditions of equilibrium from variational principles, offering a systematic and rigorous route to describe the state of the membrane. Now we provide a detailed interpretation of these results in term of stresses (mechanical point of view) and point out various subtleties associated to finding an accurate description in terms of a balance of forces. For the sake of clarity, reasonings will be performed in the simple case of a flat membrane.

Pelrine's point of view: can the electrostatic coupling be reduced to a homogeneous pressure?

We start by evaluating a common approach found in the literature on incompressible electroactive elastomers (Poisson ratio $\nu = 1/2$)[48]: it is often assumed that the electrostatic effect can be entirely reproduced by considering a pressure $2\mathcal{P}$ exerted by the electrode on the membrane, which is twice as large as the electrostatic pressure acting on a rigid plate capacitor. Considering a flat membrane, the electrostatic free energy per unit width is proportional to the covered zone l and inversely proportional to the thickness h:

$$F_U = -\frac{\varepsilon}{2}\frac{U^2 l}{h}. \tag{42}$$

The variation of the free energy F_U with respect to the two degrees of freedom h and l,

$$dF_U = \frac{\partial F_U}{\partial h}dh + \frac{\partial F_U}{\partial l}dl \tag{43}$$

reveals the resultant of the forces exerted on the electrode. The variation with respect to h gives a force normal to the electrode and equal to $\mathcal{P}l$, while the variation with respect to the length l gives a negative tension equal to $-\mathcal{P}h$, which must be a force parallel to the electrode. Noting that the free energy [Eq. (42)] is proportional to the surface, this force is analogous to a negative surface tension. Note that volume conservation implies that the two degrees of freedom are linked by $h\,dl = -l\,dh$, which means that both terms in Equation (43) are equal, hence Pelrine's doubled pressure equivalence.

To clarify the interpretation proposed by Pelrine, let us consider the case of a *compressible* elastic strip submitted to a normal stress $\mathcal{P}/\nu$ on its surface, in the absence of any electrostatic field. We can solve Hooke's elasticity equations in the membrane using $(\sigma_{ZZ} = -\mathcal{P}/\nu, \sigma_{XX} = T/H)$ and obtain

$$\frac{EH}{1-\nu^2}e_t - \frac{1}{1-\nu}H\mathcal{P} = T. \tag{44}$$

Indeed, this is the exact same equation as (33), for arbitrary ν. Hence, replacing all electrostatic effects by a mechanical pressure amplified by a coefficient $1/\nu$ with respect to the real electrostatic pressure exerted on a rigid plate capacitor, we recover the equation for the in-plane extension that was obtained rigorously through variational principle.[48] This analogy also provides the correct equation in cases where the strip is only partially covered by an electrode.

However, this interpretation is not as successful when considering the normal strain e_n. Applying an effective pressure $\mathcal{P}/\nu$ leads to

$$\frac{EH}{1-\nu^2}e_n + \frac{1}{\nu}H\mathcal{P} = -\frac{\nu}{1-\nu}T. \tag{45}$$

Comparing this to the variational result (34), one finds that the effective pressure approach does not correctly describe the normal strain e_n, except for the particular limit $\nu = 1/2$, that is, if the material is incompressible. Hence, we conclude that in the planar case the effect of electrostatics can be accounted for by an enhanced normal pressure, but only in the incompressible limit. We refer to Suo[40] for a justification of this fact based on the remark that the addition of an isotropic pressure has no effect on incompressible media.

However, even in this particular case of incompressible materials ($\nu = 1/2$), there is an additional drawback of the "double pressure" interpretation when we turn to nonplanar states. Applying a pressure $2\mathcal{P}$ on both faces of a on an element of length ds of elastic strip with a curvature κ results in a nonzero net force $2\mathcal{P}H\kappa ds$ acting along the normal $\mathbf{n}$. Defining now $\mathbf{f}$ as the internal force in the strip, the equilibrium balance on an element of length ds leads to

$$\frac{d\mathbf{f}}{ds} + 2\mathcal{P}H\kappa\mathbf{n} = 0.$$

As a consequence, this would lead to a nonconstant internal force $\mathbf{f}$, in contrast with previous results. The torque equilibrium equation (35) would also be different and simply lead to $B\theta'' + \mathbf{f}.\mathbf{n} = 0$. It does not provide the electrostatically induced added bending stiffness of the strip B_U. It is therefore not exact that all electrostatic effects can be completely replaced by a double electrostatic pressure on the faces of the electrode. This approach does not extend to geometrically nonlinear problems such as electrostatically induced buckling.

The Maxwell stress approach

To improve upon the stress-based interpretation, we now turn to a more systematic procedure to finding the distribution of electrostatic forces inside the elastic membrane. In continuum mechanics, electrostatic effects can be introduced via the Maxwell stress tensor.[41] It is defined as a tensor field whose divergence gives the electrostatic force density and reads:

$$\tau_{ij}^M = \varepsilon \frac{\partial\phi}{\partial x_i}\frac{\partial\phi}{\partial x_j} - \frac{1}{2}\varepsilon\frac{\partial\phi}{\partial x_k}\frac{\partial\phi}{\partial x_k}\delta_{ij}. \quad (46)$$

Its derivation is based on the total electrostatic force on a body, via

$$F_i = \int dV \frac{\partial\tau_{ij}^M}{\partial x_j} = \oint dA\, \tau_{ij}^M n_j. \quad (47)$$

One verifies by direct evaluation that

$$\frac{\partial\tau_{ij}^M}{\partial x_j} = \varepsilon\frac{\partial^2\phi}{\partial x_k^2}\frac{\partial\phi}{\partial x_i} = -\rho\frac{\partial\phi}{\partial x_i}, \quad (48)$$

where in the last step, we used Gauss's law and ρ is the charge density. So indeed, the divergence of τ^M gives the expected force density $-\rho\nabla\phi$.

From a mechanical perspective, the coupled electrostatic–elastic problem consists of solving

$$\frac{\partial\tau_{ij}}{\partial x_j} - \rho\frac{\partial\phi}{\partial x_i} = 0, \quad \text{or} \quad \frac{\partial}{\partial x_j}\left(\tau_{ij} + \tau_{ij}^M\right) = 0, \quad (49)$$

with appropriate boundary conditions. This provides the detailed information of the elastic stress, as well as the stress resulting from the applied electrostatic forces.

To illustrate this, we consider a flat portion of the membrane that is covered by the electrode (far away from the edge). The electrostatic field obtained in Equation (17) has only a component along z, with $\partial\phi/\partial z = U/h$. In the limit of small deformation, we replace $z \simeq Z$ and $h \simeq H$, so that the Maxwell stress tensor becomes:

$$\tau_{ZZ}^M = \frac{1}{2}\varepsilon\frac{U^2}{H^2} = \mathcal{P}, \quad \tau_{XX}^M = -\frac{1}{2}\varepsilon\frac{U^2}{H^2} = -\mathcal{P}. \quad (50)$$

Note that far away from the edges, τ^M vanishes everywhere outside the electrodes. We now compute the total membrane tension by integrating the total stress projected in the X direction, over the gap between the electrodes. This gives:

$$T = \int_{-H/2}^{H/2} \tau_{XX}^{\text{total}} dZ = \int_{-H/2}^{H/2}(\tau_{XX} + \tau_{XX}^M)dZ = H\langle\tau_{XX}\rangle - H\mathcal{P},$$
$$(51)$$

where $\langle\tau_{XX}\rangle$ is the average elastic axial stress in the membrane. Using Hooke's law and the kinematics of Equation (9), we do recover

$$T = Y[e_t + \frac{\nu}{1-\nu}e_n)] - H\mathcal{P}. \quad (52)$$

This result is strictly identical to Equation (31), and we see that the integral of the Maxwell stress gives the correct tension inside the membrane. We also recover, as previously deduced from energetics, that the elastic stress is discontinuous at the boundary of the electrode since the elastic stress obeys the standard mechanical rule $\langle\tau_{XX}\rangle = T/H$ outside the electrode. We finally note that by studying the Maxwell stress in curved geometries, we may also recover the electrostatic additional bending stiffness B_U (Appendix A1).

Given the symmetric appearance of the elastic stress τ and the Maxwell stress τ^M in Equation (49), it is tempting to give them the same interpretation—namely, as the actual distribution of elastic and electrostatic force per unit area acting on the boundary of the body. $\sigma \cdot \mathbf{n}$ gives the force of elastic origin acting through this surface, and in this spirit, the Maxwell $\sigma^M \cdot \mathbf{n}$ would give the electrostatic force (sum of the elementary charge interaction) acting on this surface. But this is not the case. For example, there are no charges in the membrane (excluding the conductors), so that no electrostatic load is directly applied through any of the surfaces—yet, the Maxwell stresses are nonzero throughout the membrane. The Maxwell stresses are therefore not the contact stresses applied by charges within the material but provide an effective representation of long-range electrostatic forces. In fact, there are different possible choices of the Maxwell stress.[41]

Force transmitted by surface charges

The actual distribution of electrostatic forces on the elastic material therefore remains to be determined. We start by considering the mechanical equilibrium of the volume enclosed by the dashed contour in Figure 2a, which involves both a part of the conductors and of the elastic membrane. The control surface separating the system from the external region is chosen along a normal to the plate, as is done standardly for the mechanical interpretation of surface tension. The boundary on the right is considered to be a free edge, free of any elastic or electrostatic forcing, so that the total tension $T = 0$. There is a resultant electrostatic force, localized in the vicinity of the left boundary. Namely, the positive charges in the upper plate inside the control volume are subjected to a force due to surface charges in both upper and lower plates outside the control volume. However, those in the upper plate are in closer proximity, so the resultant force is dominated by the repulsive interaction—as indicated by the red arrow. By symmetry, the same argument applies to the charges of the lower plate inside the control volume. When explicitly computing the integrals over the charge densities, one finds the force exerted on the upper (or lower) plate to be $\mathcal{P}H/2$ oriented to the right (Appendix A1). As $T = 0$, the total repulsive electrostatic force $\mathcal{P}H$ must be balanced by a tensile elastic stress of equal magnitude, oriented to the left (Fig. 2a, orange arrows).

Considering now the general case ($T \neq 0$, Fig. 2b), the total force across a section of the membrane (the tension) can be expressed as $T = -H\mathcal{P} + < \tau_{XX} > H$, where the direct electrostatic force $\frac{1}{2}\mathcal{P}H$ complements that transmitted from one side to the other through the elastic stress:

$$\tau_{XX} = \frac{E}{1 - \nu^2} e_t - \frac{\nu}{1 - \nu}\mathcal{P}. \tag{53}$$

The total membrane tension T consists of a bulk-elastic contribution and an electrostatic contribution localized exactly at the surface. In Figure 2b, we exemplify the case where the length of the membrane is kept unchanged that is, when $e_t = 0$. A fraction, determined by ν, of the vertical stress of electrostatic origin is redistributed horizontally, leading to an elastic contribution to the tension, due to electrostatics, but transmitted as a contact force in the bulk of the membrane (orange arrows).

Consider now the system enclosed by the very same contour, but containing only the conductors, as shown in Figure 2c. The electrostatic force exerted by the external region on the system is the same as before (red arrow). It must be balanced by an opposite force (green arrows) exerted by the membrane on the electrode, which below we show to be located at the edge.
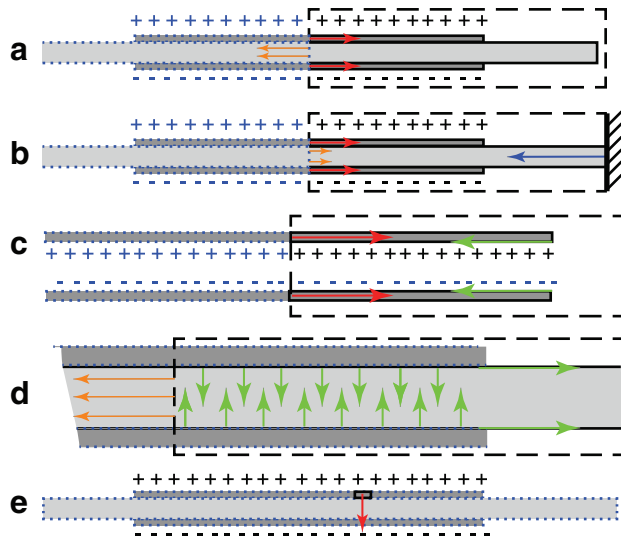
Edge effects

So far, the discussion of the electrostatic field has been simplified by avoiding the proximity of the edges of the conductor. Namely, the expressions for ϕ and the resulting elastic stress have been evaluated at distances from the edge large compared to the thickness H, avoiding fringe effects. In this thin membrane description, Equation (51) implies a discontinuity of elastic tension $H\langle\tau_{XX}\rangle$ near the conductor's edge since T is constant while $\mathcal{P}$ suddenly vanishes beyond the conductor's edge. In the light of Figure 2c, it is therefore of interest to investigate the mechanics near the edge and reveal the origin of the discontinuity.

In Figure 2d, we consider the free body diagram similar to Figure 2a, but now considering the membrane only that is, excluding the conducting plate. Hence, no surface charges are included into the control volume so that there are no Coulombian forces acting on the system. Instead, there are only contact forces that act at the boundary of the enclosed volume. From the action–reaction principle, one can infer that the normal stress exerted on the membrane is equal to the electrostatic stress (Fig. 2e). As a consequence, turning back to Figure 2d, a compressive stress of magnitude $\mathcal{P}$ is exerted on the membrane in the vertical direction. In the horizontal direction, we recall that the elastic tension on the left boundary has a magnitude $H\mathcal{P}$, pointing to the left (orange arrow in Fig. 2d). At equilibrium, this horizontal force must be balanced. However, the right side is free of elastic stress and the surface charges that gave the balance in Figure 2b can no longer come to the rescue, as these are not inside the control volume. Indeed, the only possibility is that a point force emerges at the conductor edge, as previously indicated in Figure 2c. This point force is the origin of the "discontinuity" of the elastic tension, as observed in the thin membrane description.

FIG. 2. **(a)** Distribution of forces exerted by half of the system on the other half in a situation where no external tension is applied. **(b)** Same, when an external tension is applied to prevent extension (*blue arrow*). **(c)** Electrostatic force exerted by the left part of the capacitor on the subsystem delimited by the *dashed line* (*red arrow*). The electrostatic free energy has a contribution proportional to the surface, in a close analogy with a negative surface tension. Accordingly, this energy is associated with a repulsive force in the plane of the conductors. It is balanced by an opposite force from the membrane located at the edge (*green arrow*). **(d)** Distribution of surface stress applied to the membrane (*green arrows*). The elastic tension results from the elastic stress applied on the left boundary (*orange arrows*). **(e)** The normal stress exerted by the capacitor on the elastic membrane can be determined from the action reaction principle, considering a piece of conductor as the system. Color images are available online.

How can such a point force occur? To address this question, we again change control volume—this time we consider only the electrostatic forces on the capacitor, excluding the elastic membrane. The electrostatic forces on the surface charges of the plate must be directly transmitted to the elastic membrane onto which the plate is glued (Fig. 2c). The inset of Figure 3 shows the fringe field near the edge of the plate, which can be solved analytically by conformal mapping[49,50] that is, using a change of coordinates preserving orientation and angles locally. The idea behind this analysis is to take the solution to the infinite plane capacitor and then to fold the boundary by a conformal mapping to match the boundary of the finite capacitor. The derivation is given in Appendix A1. Based on this analytical solution for ϕ, we can compute the surface charge density

$$\sigma = -\varepsilon\nabla\phi\cdot\mathbf{n}, \qquad (54)$$

where $\mathbf{n}$ is the normal pointing outward the conducting plane. Even though the solution is for an infinitely thin plate, we note that one needs to distinguish between the ''inside'' (or ''membrane side'') of the plate ($\mathbf{n}$ pointing into the membrane, blue vector in Fig. 3) and the ''outside'' ($\mathbf{n}$ pointing away from the membrane, red vector in Fig. 3). The force per unit area on the conductor will be along the normal direction and follows as

$$\tau_n = -\frac{1}{2}\sigma(\nabla\phi\cdot\mathbf{n}) = \frac{1}{2}\varepsilon|\nabla\phi|^2 = \frac{1}{2\varepsilon}\sigma^2. \qquad (55)$$

At the edge of the plate, where the normal $\mathbf{n}$ turns from upward to downward, there is indeed a singular horizontal force. In reality, conductors are not infinitely thin so that the tangential force is not a delta function but a distributed peak. More precisely, the characteristic thickness of the conductors fixes the typical size over which the tangential force is spread over space.

Let us now discuss the results from the conformal mapping discussed in Appendix A1. The exact solution for the charge density is given in a parametric form. We denote by x the
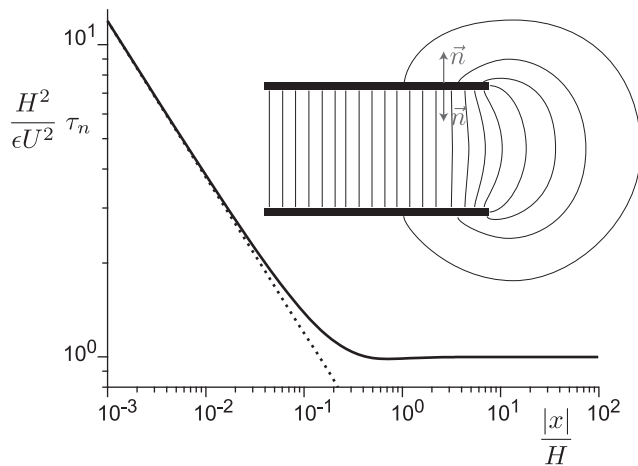

FIG. 3. Normal stress distribution as a function of the distance to the edge (*solid line*). *Dashed line* shows the analytical asymptotics. Each piece of conductor is associated with two surface charges, one above and the other below the conductor, and accordingly, with two normal unit vectors $\vec{n}$.

horizontal coordinate along the membrane and locate the right edge at $x = 0$ so that the membrane is in the half-space $x < 0$. The mapping involves the following coordinate transformation

$$x = \xi_\pm + \frac{H}{2\pi}\left(1 - e^{2\pi\xi_\pm/H}\right), \qquad (56)$$

where ξ_+ is the new (noncartesian) coordinate for the outside part of the capacitor (ξ_+ varies logarithmically with x) and ξ_- the inside part of the capacitor ($\xi_- \simeq x$ asymptotically). The exact solution for the charge density reads

$$\sigma^\pm = \pm\varepsilon\frac{U}{H}\frac{1}{1 - e^{2\pi\xi_\pm(x)}}, \qquad (57)$$

where $\sigma^\pm$ is the surface charge that resides on the exterior (+) and at the interior (−) of the plate. One verifies that both inside and outside the capacitor, σ diverges near the edge according to

$$\sigma \sim \varepsilon\frac{U}{H}\sqrt{\frac{H}{4\pi|x|}}. \qquad (58)$$

Hence, the associated normal stress, which points in opposite directions on both sides, presents a $1/|x|$ divergence,

$$\tau_n = \frac{1}{2\varepsilon}\sigma^2 \sim \varepsilon\frac{U^2}{H^2}\frac{H}{8\pi|x|}. \qquad (59)$$

One can indeed understand that such a $1/|x|$ singularity gives a finite horizontal contribution when integrating around the edge. Namely, we remind that the plate will in reality have a finite thickness that comes along with a ''rounded'' edge, providing a cutoff scale r. In this rounded section, the normal $\mathbf{n}$ has a horizontal contribution. Since furthermore the length of this section is proportional to r, the integral over stress $\tau_n \sim \varepsilon\frac{U^2}{Hr}$ will give a finite horizontal contribution $\sim \varepsilon U^2/H \sim \mathcal{P}H$. Hence, the point force indicated in Figure 2d is due to the integrable stress singularity at the conductor's edge.

Finally, we analyze the vertical force on the conductor. Inside the capacitor, we find that σ^- decays to $\varepsilon U/h$ away from the edge while outside the capacitor, σ^+ decays to 0. Since the normals are pointing in the opposite direction, the vertical stress τ_{ZZ} exerted on the electrode (and hence on the membrane) can be expressed as a difference of τ_n between both sides:

$$\tau_{ZZ} = \varepsilon\frac{U^2}{H^2}\left[\frac{1}{\left(1 - e^{2\pi\xi_-(x)}\right)^2} - \frac{1}{\left(1 - e^{2\pi\xi_+(x)}\right)^2}\right]. \qquad (60)$$

This result for τ_{ZZ}, properly normalized, is represented in Figure 3 as a function of the cartesian coordinate x. Close to the edge, the normal stress diverges as:

$$\tau_{ZZ} \sim \varepsilon\frac{U^2}{H^2}\frac{2}{3}\sqrt{\frac{H}{\pi|x|}}. \qquad (61)$$

This vertical force is a weaker singularity than for τ_n and does not lead to a point force at the edge upon integration.

Concluding Remarks

We presented a theoretical study of partially active electromembranes. We derived the equilibrium equations of an electrostatically activated beam with variational techniques. These equations were then written in an alternative way, allowing a new interpretation in terms of reference state: the electrostatic solicitation is seen as defining a new stress-free reference state. The analogy with swelling, biological growth, or plastic deformation makes this point of view particularly convenient when considering out-of-plane displacement and buckling problems. Indeed, the difficulties arising from elastic strain discontinuities (whose origin is the singular electrostatic forces at the boundary of the electrode) simply come from a difference in rest state in this equivalent framework. We also showed that Pelrine's approach, often used, that consists of considering that the electrostatic solicitation acts as a doubled pressure along the thickness of the membrane leads to the same equation for the in-plane extension. However, for polymers whose Poisson ratio differs from $1/2$, the doubled pressure does not yield the correct equation governing the normal strain. Moreover, by including geometric nonlinearities in our energetic approach, we shed light on an electrostatically induced added bending stiffness phenomenon. This feature is missing in Pelrine's approach, which also generates spurious nonbalanced pressure forces. In the second section, we clarified the intricate balance of forces in this system. In particular, we examined the question of the doubled pressure along the thickness and gave an interpretation of the Maxwell stress tensor. Finally, we considered several control contours, as is often done for surface tension problems, to understand how forces are transmitted by the charges. More precisely, by calculating the electric field at the edges of the electrode, we elucidate the major role played by the edge effects and show that it is the origin of the elastic discontinuity of the elastic stress highlighted in the previous part.

This work is pertinent for the description of geometrically nonlinear slender electroactive plates in the small strain approximation and in 2D case (elastica). It provides a better understanding of the physics of dielectric polymers that might prove useful for further developments. It remains to be generalized to more general kinematics of plates. It would be interesting to also consider the effect of large strains, which are often generated in electroactive devices. We, however, expect that the features we have presented here (e.g., singular forces at the border of the electrode leading to discontinuities in elastic strain, equivalent description in terms of a new rest state) will still be relevant in the more general case.

Author Disclosure Statement

No competing financial interests exist.

Funding Information

References

1. Ilievski F, Mazzeo AD, Shepherd RF, et al. Soft robotics for chemists. Angew Chem Int Ed 2011;50:1890–1895.
2. Shepherd RF, Ilievski F, Choi W, et al. Multigait soft robot. Proc Natl Acad Sci U S A 2011;108:20400–20403.
3. Martinez RV, Branch JL, Fish CR, et al. Robotic tentacles with three-dimensional mobility based on flexible elastomers. Adv Mater 2013;25:205–212.
4. Roche ET, Wohlfarth R, Overvelde JT, et al. A bioinspired soft actuated material. Adv Mater 2014;26:1200–1206.
5. Cheney N, Clune J, Lipson H. Evolved electrophysiological soft robots. In: ALIFE 14: The Fourteenth Conference on the Synthesis and Simulation of Living Systems, vol. 14. Cambridge, MA: MIT Press, 2014, pp. 222–229.
6. Long JH, Combes S, Nawroth J, et al. How does soft robotics drive research in animal locomotion? Soft Robot 2014;1:161–168.
7. Kato Y, Sekitani T, Takamiya M, et al. Sheet-type braille displays by integrating organic field-effect transistors and polymeric actuators. IEEE Trans Electron Dev 2007;54:202–209.
8. Pelrine R, Kornbluh R, Pei Q, et al. High-speed electrically actuated elastomers with strain greater than 100%. Science 2000;287:836–839.
9. Paul B, Qibing P. Advances in dielectric elastomers for actuators and artificial muscles. Macromol Rapid Commun 2010;31:10–36.
10. Kanda M, Gourdon R, Lancelin MJM, et al. High strain electrostrictive polymers: elaboration methods and modelization, [PhD Thesis]. Villeurbanne, France: INSA Lyon; 2011.
11. Bauer S, Bauer-Gogonea S, Graz I, et al. 25th anniversary article: a soft future: from robots and sensor skin to energy harvesters. Adv Mater 2014;26:149–162.
12. James B, Karsten D, Julia H, et al. Electroactive polymers: developments of and perspectives for dielectric elastomers. Angew Chem Int Ed 2013;52:9409–9421.
13. Kovacs G, Lochmatter P, Wissler M. An arm wrestling robot driven by dielectric elastomer actuators. Smart Mater Struct 2007;16:S306.
14. Jung K, Koo JC, do Nam J, et al. Artificial annelid robot driven by soft actuators. Bioinspir Biomim 2007;2:S42.
15. Carpi F, Rossi DD. Bioinspired actuation of the eyeballs of an android robotic face: concept and preliminary investigations, Bioinspir Biomim 2007;2:S50–S63.
16. Carpi F, Migliore A, Serra G, et al. Helical dielectric elastomer actuators. Smart Mater Struct 2005;14:1210.
17. Anderson IA, Tse T, Inamura T, et al. A soft and dexterous motor. Appl Phys Lett 2011;98:123704.
18. Jordi C, Michel S, Fink E. Fish-like propulsion of an airship with planar membrane dielectric elastomer actuators. Bioinspir Biomim 2010;5:026007.
19. Lau G-K Lim H-T, Teo J-Y, et al. Lightweight mechanical amplifiers for rolled dielectric elastomer actuators and their integration with bio-inspired wing flappers. Smart Mater Struct 2014;23:025021.
20. Giousouf M, Kovacs G. Dielectric elastomer actuators used for pneumatic valve technology. Smart Mater Struct 2013;22:104010.
21. Murray C, McCoul D, Sollier E, et al. Electro-adaptive microfluidics for active tuning of channel geometry using polymer actuators. Microfluid Nanofluid 2013;14:345–358.
22. Akbari S, Shea HR. Microfabrication and characterization of an array of dielectric elastomer actuators generating uniaxial strain to stretch individual cells. J Micromech Microeng 2012;22:045020.
23. Chakraborti P, Toprakci HK, Yang P, et al. A compact dielectric elastomer tubular actuator for refreshable Braille displays. Sens Actuat A Phys 2012;179:151–157.

24. Vishniakou S, Lewis BW, Niu X, *et al.* Tactile feedback display with spatial and temporal resolutions. Sci Rep 2013;3:2521.
25. Son S-I, Pugal D, Hwang T, *et al.* Electromechanically driven variable-focus lens based on transparent dielectric elastomer. Appl Opt 2012;51:2987–2996.
26. Maffli L, Rosset S, Ghilardi M, *et al.* Ultrafast all-polymer electrically tunable silicone lenses. Adv Funct Mater 2015; 25:1656–1665. DOI: 10.1002/adfm.201403942
27. Rossiter J, Yap B, Conn A. Biomimetic chromatophores for camouflage and soft active surfaces. Bioinspir Biomim 2012;7:036009.
28. Wang Q, Gossweiler GR, Craig SL, *et al.* Cephalopod-inspired design of electro-mechano-chemically responsive elastomers for on-demand fluorescent patterning. Nat Commun. 2014. DOI: 10.1038/ncomms5899
29. Fang ZH, Punckt C, Leung EY, *et al.* Tuning of structural color using a dielectric actuator and multifunctional compliant electrodes. Appl Opt 2010;49:6689–6696.
30. Romano P, Araromi O, Rosset S, *et al.* Tunable millimeter-wave phase shifter based on dielectric elastomer actuation. Appl Phys Lett 2014;104:024104.
31. Kaltseis R, Keplinger C, Baumgartner R, *et al.* Method for measuring energy generation and efficiency of dielectric elastomer generators. Appl Phys Lett 2011;99:162904.
32. McKay TG, O'Brien BM, Calius EP, *et al.* Soft generators using dielectric elastomers. Appl Phys Lett 2011;98:142903.
33. Foo C, Koh SJA, Keplinger C, *et al.* Performance of dissipative dielectric elastomer generators. J Appl Phys 2012; 111:094107.
34. Zhao X, Wang Q. Harnessing large deformation and instabilities of soft dielectrics: Theory, experiment, and application, Applied Phys Rev 1. 2014. DOI: 10.1063/1.4871696
35. O'Halloran A, O'Malley F, McHugh P. A review on dielectric elastomer actuators, technology, applications, and challenges. J Appl Phys 2008;104:071101.
36. Jeong-Yun S, Christoph K, Zhigang WGMS. Ionic skin. Adv Mater 2014; 26:7608–7614. DOI: 10.1002/adma.201403441
37. Bense H, Trejo M, Reyssat E, *et al.* Buckling of elastomer sheets under non-uniform electro-actuation. Soft Matter 2017;13:2876–2885.
38. Li K, Wu W, Jiang Z, *et al.* Voltage-induced wrinkling in a constrained annular dielectric elastomer film. J Appl Mech 2017;85:011007.
39. Zhu R, Wallrabe U, Woias P, *et al.* Semi-rigid ring-shaped electrode dielectric electroactive polymer membrane as buckling actuator. J Micromech Microeng 2019;29:055001.
40. Suo Z. Theory of dielectric elastomers. Acta Mech Solida Sin 2010;23:549–578.
41. Dorfmann L, Ogden R. Nonlinear Theory of Electroelastic and Magnetoelastic Interactions. Bücher, Springer US: SpringerLink, 2014.
42. Greaney P, Meere M, Zurlo G. The out-of-plane behaviour of dielectric membranes: Description of wrinkling and pull-in instabilities. J Mech Phys Solids 2019;122:84–97.
43. Audoly B, Pomeau Y. Elasticity and Geometry: From Hair Curls to the Nonlinear Response of Shells. Oxford, United Kingdom: Oxford University Press, 2010.
44. Landau LD, Lifshitz EM, Pitaevskii LP. Electrodynamics of Continuous Media. Oxford, United Kingdom: Butterworth-Heinemann, 1984.
45. de Gennes P-G, Brochard-Wyart F, Quere D. Capillarity and Wetting Phenomena: Drops, Bubbles, Pearls, Waves. New York: Springer, 2003.
46. Lippmann G. Relations Entre les Phenomenes Electriques et Capillaires. PhD Thesis, Faculté des Sciences de Paris, 1875.
47. Love. A Treatise on the Mathematical Theory of Elasticity. Dover, Mineola, NY: 1944.
48. Ronald P, Roy K, Jose J. Electrosctriction of polymer dielectrics with compliant electrodes as a means of actuation. Sens Actuat A 1998;64:77–85.
49. Vanderlinde J. Classical Electromagnetic Theory, vol. 145. Berlin/Heidelberg, Germany: Springer Science & Business Media, 2006.
50. Valluri SR, Jeffrey DJ, Corless RM. Some applications of the lambert w function to physics. Can J Phys 2000;78:823–831.
51. Veberič D. Lambert w function for applications in physics. Comput Phys Commun 2012;183:2622–2628.
52. Feynman R, Leighton R, Sands M, *et al.* The Feynman Lectures on Physics, vol. III, vol. 33. College Park, MD: AAPT, 1965.

Address correspondence to:
Bruno Andreotti
Laboratoire de Physique de l'Ecole Normale
Supérieure (LPENS)
ENS, Université PSL, CNRS Sorbonne
Université
Université de Paris
24 Rue Lhomond F-75005
Paris
France

E-mail: andreotti@lps.ens.fr

Appendix

Appendix A1

A Conformal Mapping to Solve Electrostatics

Definitions

We now zoom at a scale comparable to H, sending consequently the size of the capacitors to infinity. Although one can use again the Green theorem, we will proceed through a conformal mapping. The 2D space is characterized by the complex coordinate $z = x + iy$. We define the complex potential

$$w(z) = \psi(x, y) + i\phi(x, y), \qquad (62)$$

where $\phi(z)$ the electrostatic potential. The lines of iso-ψ are orthogonal to lines of iso-ϕ, similar to the stream function and potential in ideal flow. On the domain where $w(z)$ is

holomorphic, the functions ψ and ϕ are harmonic and satisfy the Cauchy–Riemann equations. Hence, we can write

$$\frac{dw}{dz} = \frac{\partial \phi}{\partial y} + i \frac{\partial \phi}{\partial x} = -E_y - iE_x. \tag{63}$$

On a conductor, the density of charges reads

$$\sigma = -\varepsilon \nabla \phi \cdot \mathbf{n}, \tag{64}$$

and $\nabla \phi$ is in the normal direction. Hence, the normal force per unit area can be computed as

$$\left(-\frac{1}{2} \sigma \nabla \phi \right) \cdot \mathbf{n} = \frac{1}{2} \varepsilon |\nabla \phi|^2 = \frac{1}{2} \varepsilon \left| \frac{dw}{dz} \right|^2. \tag{65}$$

Conformal mapping

We consider the solution of the infinite plane capacitor, in the plane $\zeta = \xi + i\eta$. We allow η to vary from $-h/2$ to $h/2$, with boundary conditions $\phi = \pm U/2$. The solution of course reads $\phi = U\eta/h$, which in terms of the complex potential gives

$$w(\eta) = \frac{U\zeta}{h}. \tag{66}$$

One verifies $dw/d\zeta = U/h$, so as expected $E_y = -U/h$ and $E_x = 0$. Now we perform a mapping from the ζ-plane to the physical plane of interest, defined by $z = x + iy$, according to Veberič[51]

$$z = \zeta + \frac{h}{2\pi} \left(1 + e^{2\pi\zeta/h} \right). \tag{67}$$

We verify below that this folds the conductors at $\eta = \pm h/2$ for $\xi > 0$ onto the same conductors in the range $\xi < 0$. Now, we use that $\zeta/h = w/U$, so that we find

$$\frac{z}{h} = \frac{w}{U} + \frac{1}{2\pi} \left(1 + e^{2\pi w/U} \right). \tag{68}$$

This is a closed form solution $w(z)$ as defined by its inverse. The properties of the field and the charge density are encoded in the derivative

$$\frac{dw}{dz} = \frac{dw}{d\zeta} \frac{d\zeta}{dz} = \frac{U}{h} \frac{d\zeta}{dz}. \tag{69}$$

So, we can derive all results of interest from the map $z(\zeta)$ defined by Equation (67). For simplicity, we set $h = 1$, so that

$$z = \zeta + \frac{1}{2\pi} \left(1 + e^{2\pi\zeta} \right). \tag{70}$$

We find that

$$\frac{dz}{d\zeta} = 1 + e^{2\pi\zeta}. \tag{71}$$

Singularities are encountered at when the derivative vanishes, which are found at $\zeta = \pm i/2$ (we remind that η is restricted between $-1/2$ and $1/2$). Indeed, these correspond to

the plate edges $z = \pm i/2$. This means that the field strength (scaled on U/h) reads

$$\frac{d\zeta}{dz} = \frac{1}{1 + e^{2\pi\zeta}}, \tag{72}$$

and indeed diverges at the edges. To analyze the nature of the singularity, we expand the result $\zeta = i/2$, which gives

$$\frac{d\zeta}{dz} \sim \frac{1}{\zeta - \frac{i}{2}}. \tag{73}$$

Expanding the mapping around the point gives

$$z - \frac{i}{2} = -\pi(\zeta - \frac{i}{2})^2, \tag{74}$$

so that the singularity can be written as

$$\frac{d\zeta}{dz} \sim \frac{1}{(z - \frac{i}{2})^{1/2}}. \tag{75}$$

At the plate, we can write $z = x + i/2$, so that

$$\left. \frac{d\zeta}{dz} \right|_{up} \sim \frac{1}{x^{1/2}}. \tag{76}$$

This implies that the field, and thus the surface charge, diverges as $1/x^{1/2}$. Next, we write the equations in terms of the real coordinates as:

$$x = \xi + \frac{1}{2\pi} \left(1 + e^{2\pi\xi} \cos 2\pi\eta \right), \tag{77}$$

$$y = \eta + \frac{1}{2\pi} e^{2\pi\xi} \sin 2\pi\eta. \tag{78}$$

The upper plate is located at $\eta = 1/2$. The relationship between x and ξ is not bijective and we well therefore note $\xi_\pm(x)$ the two branches of solution corresponding to the upper and lower side of the plate.

$$x = \xi_\pm + \frac{1}{2\pi} \left(1 - e^{2\pi\xi_\pm} \right), \tag{79}$$

$$y = \frac{1}{2}. \tag{80}$$

For large negative values of ξ, one finds $\xi_- \simeq x$ (inside capacitor), while for large positive values, one finds $\xi_+ \simeq \ln(-2\pi x)/(2\pi)$ (outside capacitor, folded from $\xi > 0$). As mentioned, the field is given by

$$\frac{d\zeta}{dz} = \frac{1}{1 + e^{2\pi\zeta}} = \frac{1}{1 + e^{2\pi(\xi + i\eta)}}, \tag{81}$$

which can be seen as a function of x and y by the inverse of Equation (78). At the upper plate, $\eta = 1/2$, this reduces to

$$\frac{d\zeta}{dz} = \frac{1}{1 - e^{2\pi\xi_\pm(x)}}. \tag{82}$$

(Appendix continues →)

Negative Surface Tension Through the Coulomb Law

To determine the electrostatic force exerted on the subsystem chosen in Figure 2a by the rest of the electrodes, we introduce the Green function $-\ln(r/h)/2\pi\varepsilon$ of the electrostatic interaction in the planar problem.[52] We focus here on the infinitely extended plane capacitor, with a uniform surface charge $\pm\sigma$ at $y = \pm h/2$. Evaluated at the top electrode $n = h/2$, we find the potential

$$
\begin{aligned}
\frac{U}{2} \equiv \phi(x, h/2) &= -\sigma \int_{-\infty}^{\infty} dx' \frac{1}{2\pi\varepsilon} \ln\left(\frac{(x-x')^2}{h^2}\right) \\
&\quad + \sigma \int_{-\infty}^{\infty} dx' \frac{1}{2\pi\varepsilon} \ln\left(\frac{(x-x')^2 + h^2}{h^2}\right) \\
&= \frac{\sigma}{2\pi\varepsilon} \int_{-\infty}^{\infty} dx' \ln\left(\frac{x'^2 + h^2}{x'^2}\right) = \frac{\sigma h}{2\varepsilon}.
\end{aligned}
\tag{83}
$$

We therefore recover the standard law $\sigma = \varepsilon \nabla \phi \cdot \mathbf{n}$, which gives $\sigma = \varepsilon U/h$ for a plane capacitor.

We now divide the membrane into two parts and determine the distribution of forces exerted by one side on the other. The horizontal component of the electric field due to the other half membrane therefore reads:

$$
\partial_x V_{\frac{1}{2}}(x, y) = \frac{\sigma}{4\pi\varepsilon} \ln\left(\frac{x^2 + (h-y)^2}{x^2 + y^2}\right).
\tag{84}
$$

The electric potential induced by half a capacitor as:

$$
V_{\frac{1}{2}}(x, y) = \frac{\sigma}{4\pi\varepsilon} \int_{0}^{\infty} dx' \ln\left(\frac{(x-x')^2 + (h-y)^2}{(x-x')^2 + y^2}\right).
\tag{85}
$$

On the capacitor ($y = 0$), we get:

$$
V_{\frac{1}{2}}(x, 0) = \frac{\sigma h}{4\pi\varepsilon} \left[\frac{x}{h} \ln(1 + h^2/x^2) - 2\tan^{-1}\left(\frac{h}{x}\right)\right].
\tag{86}
$$

The horizontal repulsive force (the opposite of the tension T_U) exerted by one side on the other of the form:

$$
-T_U = \sigma\left[V_{\frac{1}{2}}(0,0) - V_{\frac{1}{2}}(\infty, 0)\right] = \frac{\sigma^2 H}{4\varepsilon} = \frac{\varepsilon}{4}\frac{U^2}{H} = \frac{\mathcal{P} H}{2}.
\tag{87}
$$

Electrostatic Bending Stiffness Computed from the Maxwell Stress Tensor

We may also compute the effective bending stiffness from electrostatic origin using the Maxwell stress tensor defined in Equation (46). From the potential computed in a curved capacitor [Eq. (17)], we deduce the Maxwell stress tensor component

$$
\tau_{XX}^M = -\frac{\varepsilon}{2}\frac{U^2}{h^2}[1 + Z\kappa]^2 = -\frac{\varepsilon}{2}\frac{U^2}{h^2}[1 + 2Z\kappa]
\tag{88}
$$

at linear order in κ. This lead to a total torque (per unit width)

$$
\begin{aligned}
M &= \int_{Z=-h/2}^{Z=h/2} \left(\sigma_{XX} + \tau_{XX}^M\right) Z dZ = \\
&\quad -B\kappa - \varepsilon\frac{U^2}{h^2}\left[\frac{h^3}{12}\kappa\right] = -(B + B_U)\kappa,
\end{aligned}
\tag{89}
$$

where we have computed the elastic stress σ_{XX} from Hooke's law and the strains defined in Equation (9). We have therefore recovered the electrostatically induced additional bending stiffness B_U with the same expression as in Equation (22).